Supplemental Material

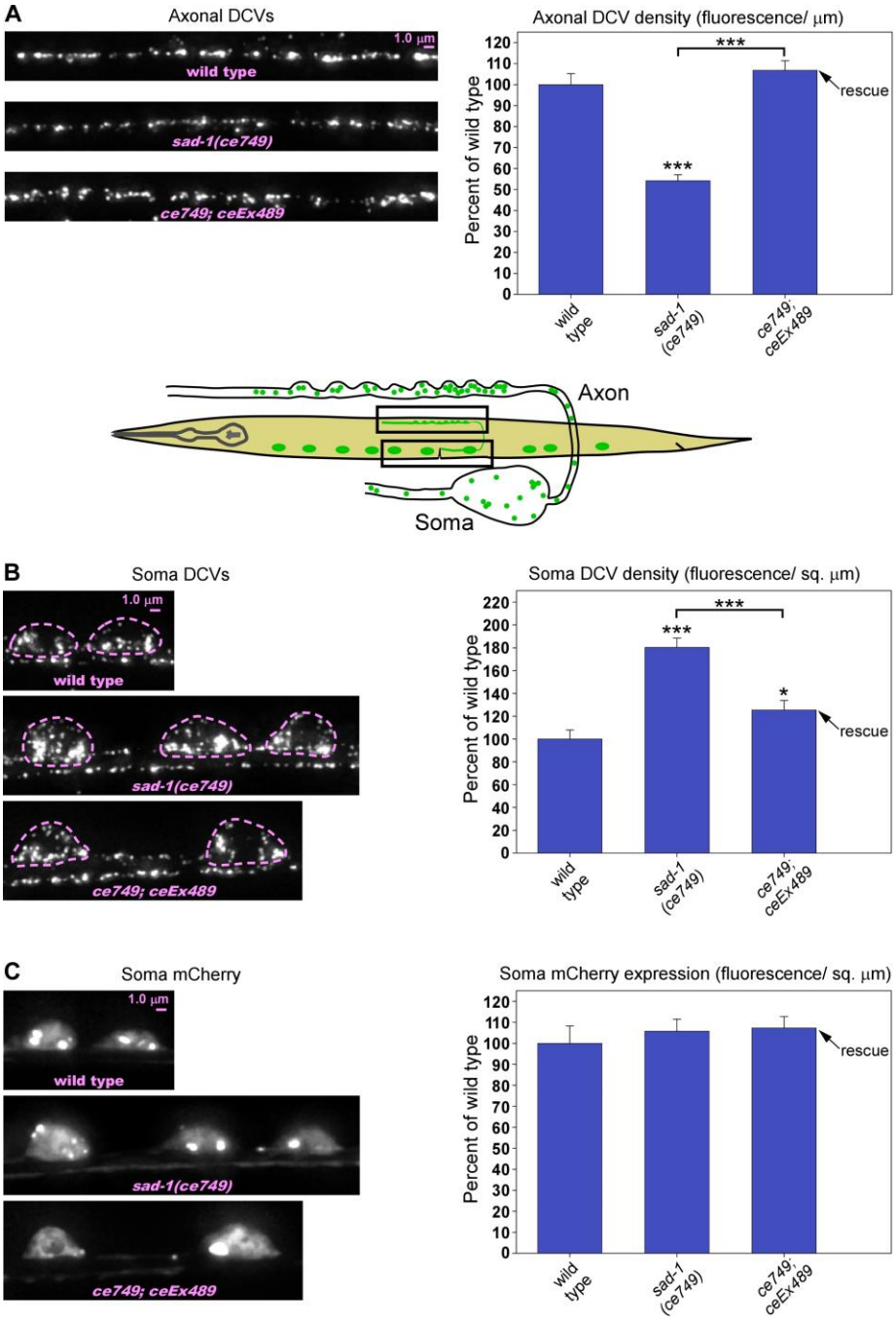

Figure S1. SAD-1 regulates DCV trafficking cell autonomously in ventral cord cholinergic neurons (related to Figure 2).

(A-C) Rectangles in drawing indicate regions imaged. Representative images and quantification of DCV or soluble mCherry fluorescence in axons and somas in the indicated genotypes. The DCV marker INS-22-Venus (a tagged neuropeptide) and mCherry are expressed from the integrated transgene *ceIs201* using the same promoter. mCherry thus provides an internal control for changes in expression. Images are identically scaled. Dashed lines in **(B)** outline cell somas. Graph data are means and standard errors from 13-15 animals each. Unmarked bars are not significantly different from wild type. * and *** indicate P-values that are <.05 or <.001, respectively. Asterisks that are not above relationship bars compare the indicated bar to wild type.

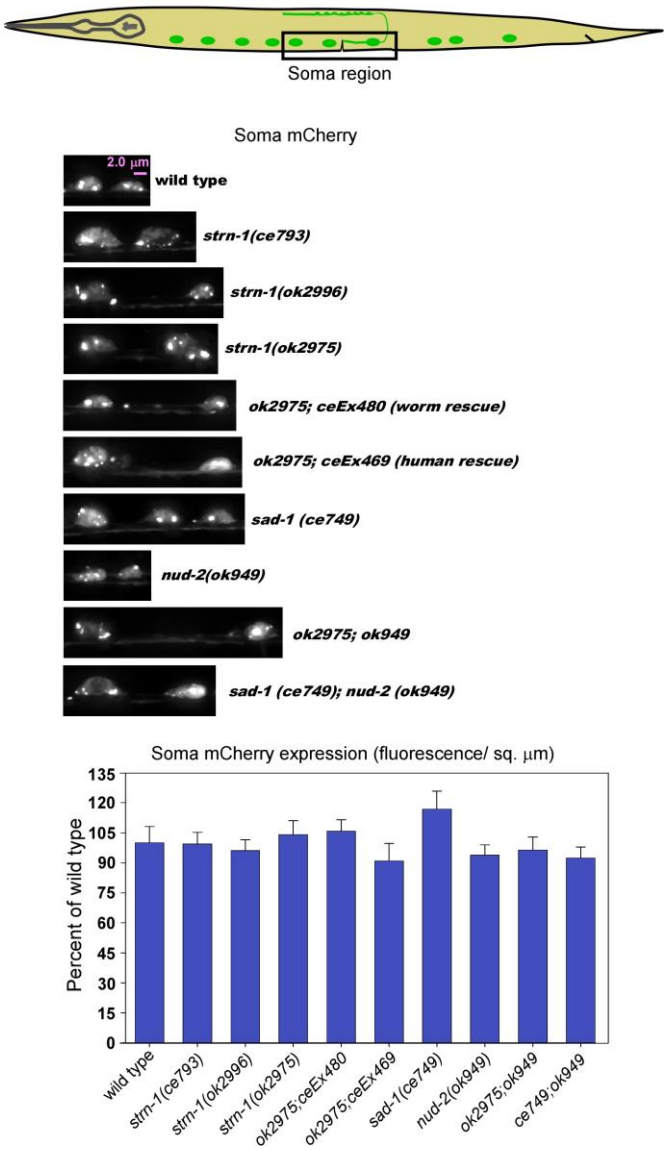

Figure S2. mCherry expression controls for strains used in Figures 2 and 3 and Figure S3.

Rectangle in drawing indicates region imaged. Representative images and quantification of mCherry fluorescence in ventral somas in the indicated genotypes. mCherry, used as an expression control, is co-expressed with the DCV marker INS-22-Venus from the integrated transgene *ceIs201*. mCherry and the DCV marker are driven by the same promoter, so mCherry provides and internal control for changes in expression. Images are identically-scaled. Graph data are means and standard errors from 13-15 animals each. Mutant means are not significantly different from wild type.

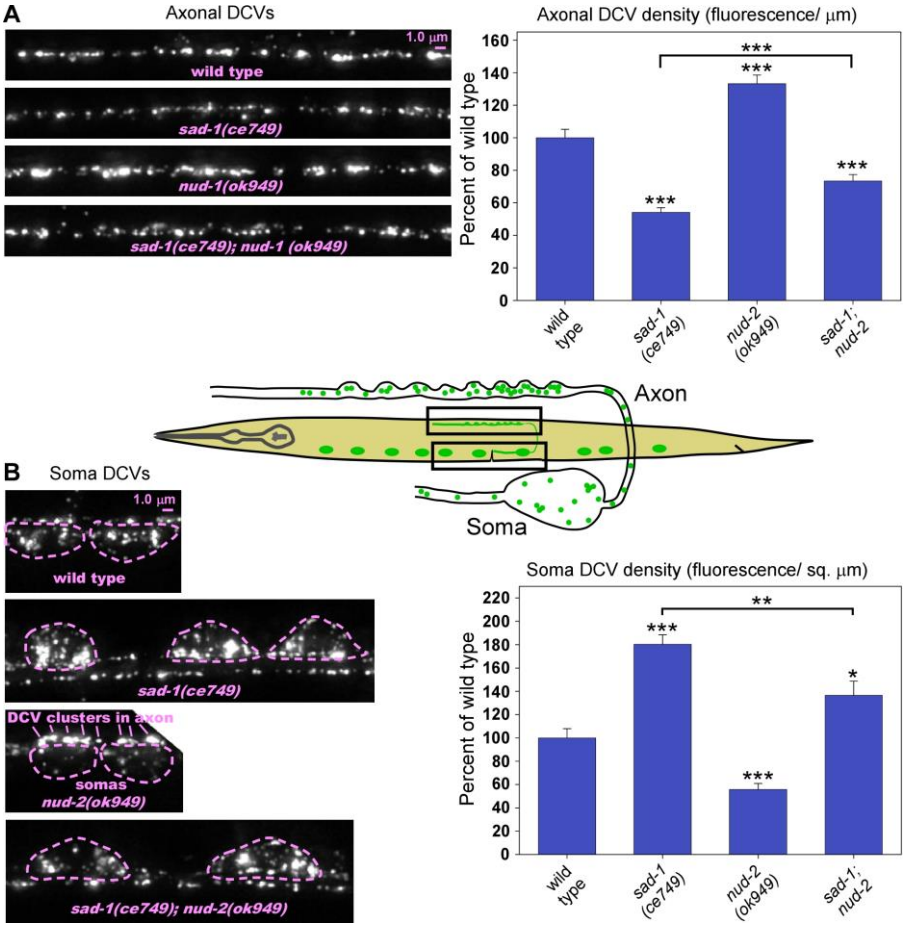

Figure S3. The altered distribution of DCVs in mutants lacking Sentryn occurs in a dynein-dependent manner (related to Figure 3).

(A-B) Rectangles in drawing indicate regions imaged. Representative images and quantification of DCV fluorescence in axons **(A)** and somas **(B)** in the indicated genotypes. The DCV marker INS-22-Venus (a tagged neuropeptide) is expressed from the integrated transgene *ceIs201*. Images are identically-scaled. Dashed lines in **(B)** outline cell somas. Graph data are means and standard errors from 13-17 animals each. Bars without asterisks are not significantly different from wild type. *, **, and *** indicate P-values that are <.05, <.01, or <.001, respectively. Asterisks that are not above relationship bars compare the indicated bar to wild type. See Figure S2 for soluble mCherry expression controls.

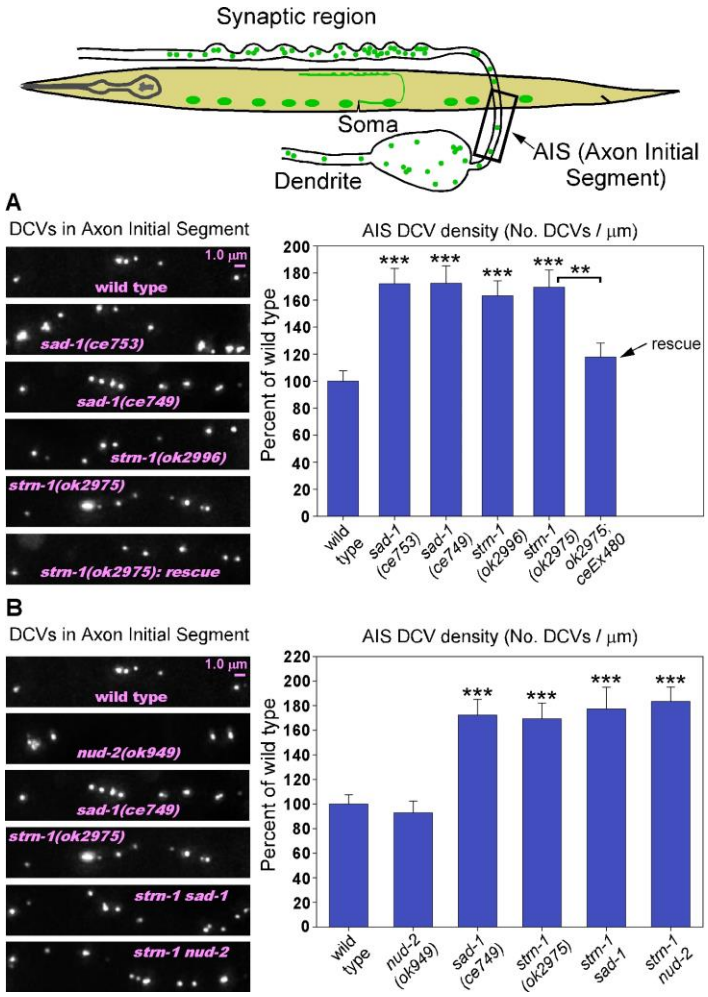

Figure S4. Mutants lacking Sentryn or SAD-1 accumulate DCVs in the axon initial segment in a dynein-independent manner (related to Figure 4).

(A-B) Representative images and quantification of DCV number/ µm in the indicated genotypes. The DCV marker INS-22-Venus is expressed from the integrated transgene array *ceIs201*. Graph data are means and standard errors from 14-15 animals each. Bars without asterisks are not significantly different from wild type. *, **, and *** indicate P-values that are <.05, <.01, or <.001, respectively. Asterisks that are not above relationship bars compare the indicated bar to wild type.

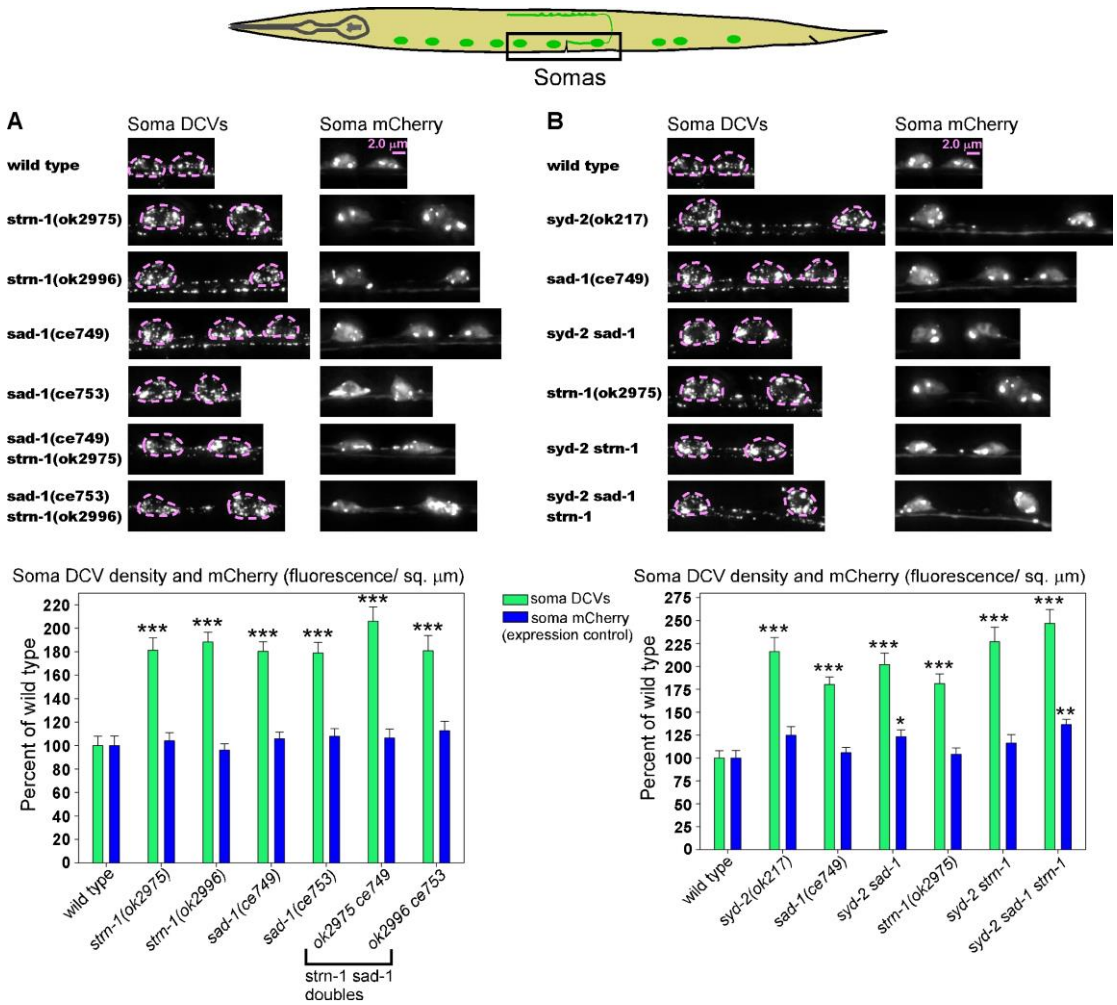

Figure S5. DCVs and mCherry (expression control) in the somas of strains used in Figure 6.

(A-B) Rectangle in drawing indicates regions imaged. Representative images and quantification of DCV or mCherry (expression control) fluorescence in ventral somas in the indicated genotypes. The DCV marker INS-22-Venus (a tagged neuropeptide) and mCherry are co-expressed from the integrated transgene *ceIs201* using the same promoter. Images are identically-scaled. Dashed lines in **(A-B)** outline cell somas. Graph data are means and standard errors from 13-17 animals each. Unmarked bars are not significantly different from wild type. *, **, and *** indicate P-values that are <.05, <.01, or <.001, respectively, and compare the indicated bar to wild type. The small, but significant, increases in mCherry expression in the *syd-2 sad-1* double and the *syd-2 sad-1 strn-1* triple, would not impact the conclusions of the experiment.

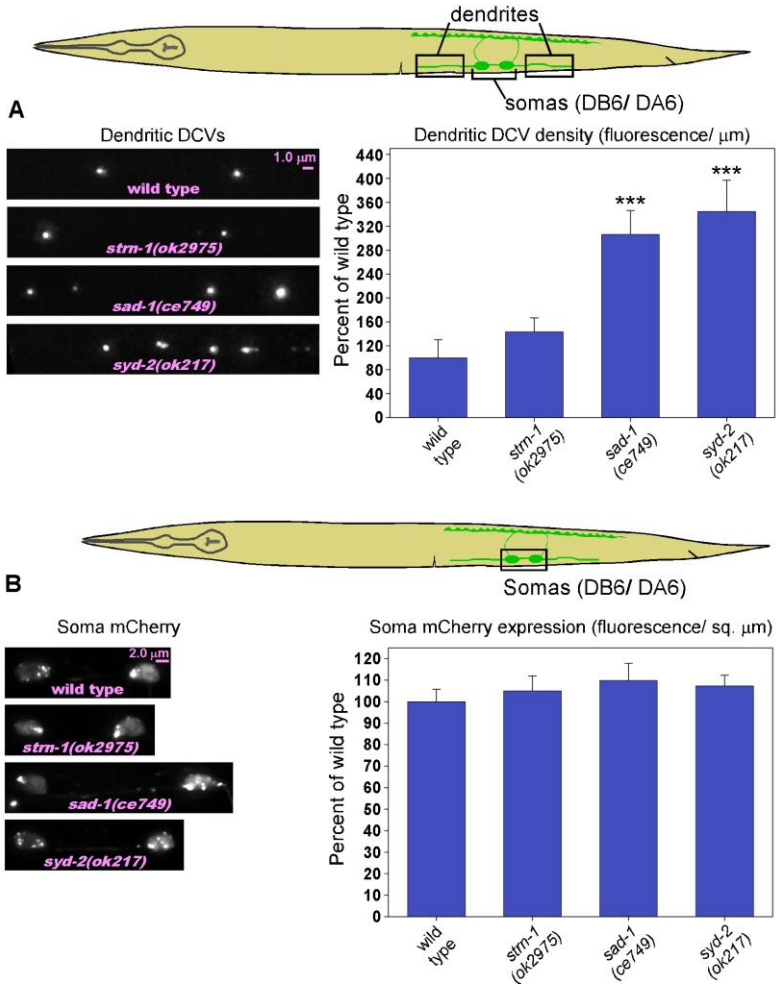

Figure S6. Unlike SAD-1 and SYD-2, Sentryn is not required to prevent over-accumulation of DCVs in dendrites (related to Figure 7).

(A) Rectangles show regions imaged. Representative images and quantification of DCV fluorescence in dendrites in the indicated genotypes. The DCV marker INS-22-Venus (a tagged neuropeptide) is expressed from the integrated transgene *ceIs255*. **(B)** shows representative images and quantification of soluble mCherry in cell somas of the indicated genotypes. Soluble mCherry is also expressed from the *ceIs255* transgene using the same promoter as the DCV marker to provide an internal control for changes in expression. Note that no changes in expression were observed. Unmarked bars are not significantly different from wild type. *** indicate P-values that are <.001.

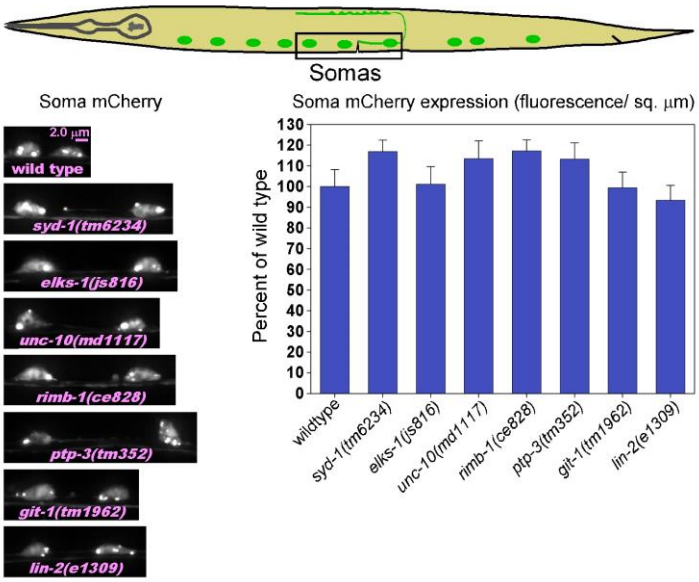

Figure S7. mCherry expression controls for strains used in Figure 7.

Rectangles in drawing indicates regions imaged. Representative images and quantification of mCherry (expression control) fluorescence in ventral somas in the indicated genotypes. mCherry is expressed from the integrated transgene *ceIs201* using the same promoter that was used for the DCV marker to provide an internal control for changes in expression. Graph data are means and standard errors from 13-15 animals each. Unmarked bars are not significantly different from wild type.

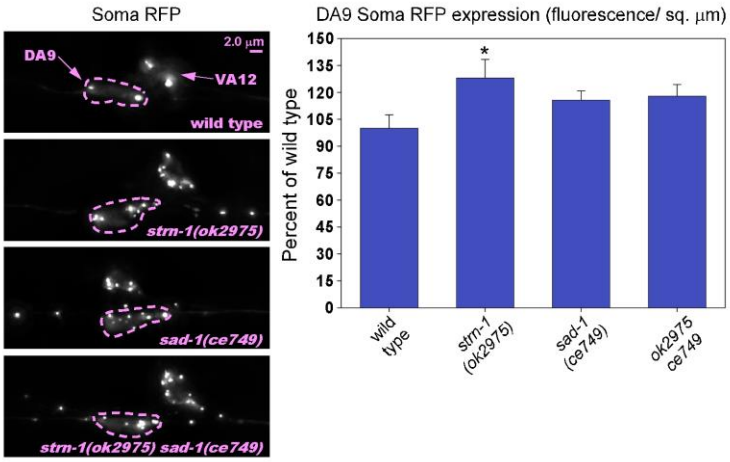

Figure S8. RFP (expression controls) in *strn-1*, *sad-1*, and double in DA9 somas (related to Figure 8).

Representative images and quantification of RFP (expression control) fluorescence in ventral somas in the indicated genotypes. The RFP is co-expressed with the INS-22-Venus DCV marker from the integrated transgene *ceIs308*. Both markers use the same promoter, so RFP expression serves as an internal expression control. Images are identically-scaled. Dashed lines outline DA9 cell somas. The VA12 soma, indicated in the wild type images, is also present in all images. Graph data are means and standard errors from 13-15 animals each. Unmarked bars are not significantly different from wild type. * indicates a P-value that is <.05 for comparing the indicated bar to wild type. The small, but significant increase of RFP expression in the *strn-1* single mutant would not impact the conclusions drawn from the data in Figure 8.

Table S1. Non-wild type *C. elegans* strains

Strain name	Genotype (origin and/ or first use cited if not produced in this study)
KG4789	*ceEx461 [strn-1::GFP]*
KG2882	*ceIs123 [unc-129::GFP]* (Hoover et al., 2014)
KG4247	*ceIs201 [unc-17::INS-22-Venus, unc-17::RFP, unc-17::ssmCherry]* (Hoover et al., 2014)
KG4664	*ceIs255 [unc-129::INS-22-Venus, unc-129::mCherry, unc-129::ssmCherry]* (Edwards et al., 2015b)
KG5082	*ceIs308 [mig-13::INS-22-Em, mig-13::RFPA]*
KG4845	*elks-1(js816); ceIs201 [unc-17::INS-22-Venus, unc-17::RFP, unc-17::ssmCherry]*
KG5033	*git-1(tm1962); ceIs201 [unc-17::INS-22-Venus, unc-17::RFP, unc-17::ssmCherry]*
KG5012	*lin-2(e1309); ceIs201 [unc-17::INS-22-Venus, unc-17::RFP, unc-17::ssmCherry]*
KG4585	*nud-2(ok949) ceIs201 [unc-17::INS-22-Venus, unc-17::RFP, unc-17::ssmCherry]*
KG5016	*ptp-3(tm352); ceIs201 [unc-17::INS-22-Venus, unc-17::RFP, unc-17::ssmCherry]*
KG5028	*rimb-1(ce828); ceIs201 [unc-17::INS-22-Venus, unc-17::RFP, unc-17::ssmCherry]*
KG4400	*sad-1(ce749)* [2X outcrossed] (Edwards et al., 2015a)
KG4941	*sad-1(ce749); ceIs123 [unc-129::GFP]*
KG4414	*sad-1(ce749); ceIs201 [unc-17::INS-22-Venus, unc-17::RFP, unc-17::ssmCherry]*
KG4991	*sad-1(ce749); ceIs201 [unc-17::INS-22-Venus, unc-17::RFP, unc-17::ssmCherry]; ceEx489 [unc-17::sad-1 cDNA]*
KG4824	*sad-1(ce749); ceIs255 [unc-129::INS-22-Venus, unc-129::mCherry, unc-129::ssmCherry]*
KG5111	*sad-1(ce749); ceIs308 [mig-13::INS-22-Em, mig-13::RFPA]*
KG5240	*sad-1(ce749); nud-2(ok949); ceIs201 [unc-17::INS-22-Venus, unc-17::RFP, unc-17::ssmCherry]*
KG4947	*sad-1(ce753); ceIs201 [unc-17::INS-22-Venus, unc-17::RFP, unc-17::ssmCherry]*
KG4319	*sad-1(ce776); ceIs201 [unc-17::INS-22-Venus, unc-17::RFP, unc-17::ssmCherry]*
KG4382	*sad-1(ce776); dpy-11(e224); ceIs201 [unc-17::INS-22-Venus, unc-17::RFP, unc-17::ssmCherry]*
KG4357	*sad-1(ce784); ceIs201 [unc-17::INS-22-Venus, unc-17::RFP, unc-17::ssmCherry]*
KG4896	*strn-1(ce793); ceIs201 [unc-17::INS-22-Venus, unc-17::RFP, unc-17::ssmCherry]* [2X outcrossed]
KG4932	*strn-1(ok2975)* [4X outcrossed]
KG4490	*strn-1(ok2996)* [4X outcrossed]
KG4887	*strn-1(ok2975); ceIs123 [unc-129::GFP]*
KG4786	*strn-1(ok2975); ceIs201 [unc-17::INS-22-Venus, unc-17::RFP, unc-17::ssmCherry]*
KG4820	*strn-1(ok2975); ceIs201 [unc-17::INS-22-Venus, unc-17::RFP, unc-17::ssmCherry]; ceEx469 [unc-17::STRN-1-Hs]*
KG4899	*strn-1(ok2975); ceIs201 [unc-17::INS-22-Venus, unc-17::RFP, unc-17::ssmCherry]; ceEx480 [unc-17::STRN-1]*
KG4794	*strn-1(ok2975); ceIs255 [unc-129::INS-22-Venus, unc-129::mCherry, unc-129::ssmCherry]*
KG5110	*strn-1(ok2975); ceIs308 [mig-13::INS-22-Em, mig-13::RFPA]*
KG4904	*strn-1(ok2975); nud-2(ok949) ceIs201 [unc-17::INS-22-Venus, unc-17::RFP, unc-17::ssmCherry]*
KG4833	*strn-1(ok2975) sad-1(ce749)*
KG4933	*strn-1(ok2996) sad-1(ce749)*
KG4945	*strn-1(ok2975) sad-1(ce749); ceIs123 [unc-129::GFP]*
KG4847	*strn-1(ok2975) sad-1(ce749); ceIs201 [unc-17::INS-22-Venus, unc-17::RFP, unc-17::ssmCherry]*
KG5112	*strn-1(ok2975) sad-1(ce749); ceIs308 [mig-13::INS-22-Em, mig-13::RFPA]*
KG4848	*strn-1(ok2975) syd-2(ok217); ceIs201 [unc-17::INS-22-Venus, unc-17::RFP, unc-17::ssmCherry]*
KG4988	*strn-1(ok2975) syd-2(ok217) sad-1(ce749); ceIs201 [unc-17::INS-22-Venus, unc-17::RFP, unc-17::ssmCherry]*
KG4430	*strn-1(ok2996); ceIs201 [unc-17::INS-22-Venus, unc-17::RFP, unc-17::ssmCherry]*
KG4978	*strn-1(ok2996) sad-1(ce753); ceIs201 [unc-17::INS-22-Venus, unc-17::RFP, unc-17::ssmCherry]*
KG5006	*syd-1(tm6234); ceIs201 [unc-17::INS-22-Venus, unc-17::RFP, unc-17::ssmCherry]*
KG4828	*syd-2(ok217); ceIs201 [unc-17::INS-22-Venus, unc-17::RFP, unc-17::ssmCherry]*
KG4725	*syd-2(ok217); ceIs255 [unc-129::INS-22-Venus, unc-129::mCherry, unc-129::ssmCherry]* (Edwards et al., 2015b)
KG4977	*syd-2(ok217) sad-1(ce749); ceIs201 [unc-17::INS-22-Venus, unc-17::RFP, unc-17::ssmCherry]*
KG4979	*unc-10(md1117); ceIs201 [unc-17::INS-22-Venus, unc-17::RFP, unc-17::ssmCherry]*

Table S2. Mutation lesions and methods used for genotyping in strain constructions

Mutation	Description of Molecular Lesion	Method(s) used for genotyping	References
elks-1(js816)	494 bp deletion within exon 6. Splicing of remaining exon creates a frameshift that results in a stop codon at amino acid 292 (out of 837 amino acids).	PCR with primers inside deleted region	(Deken et al., 2005)
git-1(tm1962)	483 bp deletion and 23 bp insertion beginning in intron 7, including all of exons 8 and 9, and ending in intron 9. Splicing of exon 7 to exon 10 creates a frameshift that results in a stop at amino acid 318 (out of 670 amino acids).	PCR with primers inside deleted region	Japanese National Bioresource Project for the Experimental Animal "Nematode *C. elegans*" and (Patel et al., 2006)
lin-2(e1309)	Not published.	Vulvaless and Egl-D phenotypes	(Ferguson and Horvitz, 1985)
nud-2(ok949)	1109 bp deletion and a 1 bp insertion. Starts at the predicted ATG of nud-2 and deletes the entire open reading frame except the last part of the last exon.	PCR with primers inside deleted region	*C. elegans* Gene Knockout Consortium and (Fridolfsson et al., 2010)
ptp-3(tm352)	506 bp deletion beginning in exon 7, including all of exons 8 and 9, and ending in exon 10 of the "a" isoform. Splicing of the remaining portions of exons 7 and 10 creates a frameshift that results in a stop at amino acid 357 (out of 2180 amino acids). Changes/ eliminates 83.7% of the total protein.	PCR with primers inside deleted region	Japanese National Bioresource Project for the Experimental Animal "Nematode *C. elegans*" and (Ackley et al., 2005)
rimb-1(ce828)	13 bp insertion after AA16 (out of 1276 AA total) introduced through oligo templated Cas9 homologous recombination. Insert contains 3 stop codons, each in a different reading frame as well as an Nhe I site for screening.	Make 542 bp PCR product centered on the insertion, followed by restriction digest with Nhe I (the insertion creates an Nhe I site). Confirm using PCR followed by sequencing.	This study
sad-1(ce749)	Q57Stop (out of 835 or 914 amino acids, depending on the isoform). Mutation position is the same in both isoforms.	Make 250 bp PCR product centered on the mutation, followed by restriction digest with Mse I (the mutation creates an Mse I site).	(Edwards et al., 2015a)
sad-1(ce753)	R147Stop nonsense mutation	Make 500 bp PCR product centered on the mutation, followed by restriction digest with Bst UI (site is only present in wild type).	(Edwards et al., 2015a)
sad-1(ce776)	E280Stop nonsense mutation	Not used in crosses	This study
sad-1(ce784)	Putative splicing mutation. Mutates the 8th intron of the "a" isoform near the splice. In wild type, it is gtgggataaaatgcatttt, which is not a great consensus after the gt (G-24%; G-9%) (Blumenthal). In the mutant it is gtgggat**ctgc**tgcatttt (changed from aaaa in wild type). The "C" at position +8 has a consensus of 9% (Blumenthal and Steward, 1997). GC (at positions 10-11 of the mutant) is sometimes rarely used as a 5' splice donor site and the att at positions 4-6 after that might enhance the site to cause mis-splicing (Blumenthal and Steward, 1997).	Not used in crosses	This study
strn-1(ok2975)	558 bp deletion and 49 bp insertion that causes a frameshift resulting in R178Stop (out of 457 amino acids). Changes/ eliminates approximately 72.5% of the protein.	PCR with primers inside deleted region	*C. elegans* Gene Knockout Consortium and this study
strn-1(ok2996)	699 bp deletion with single bp (A) insertion. A97D and amino acids 98-222 (out of 457) are deleted; then the same reading frame resumes. Affects approximately 27.5% of the protein.	PCR with primers inside deleted region	*C. elegans* Gene Knockout Consortium and this study
syd-1(tm6234)	1266 bp deletion starting in the intron between exons 7 and 8 and ends in the middle of exon 11 of the "b" isoform. The deletion eliminates R249 – Y471 (out of 942 amino acids total) and results in a frame shift predicted to prevent translation of the remaining protein.	Behavioral phenotypes and PCR with primers inside deleted region	Japanese National Bioresource Project for the Experimental Animal "Nematode *C. elegans*" and (Edwards et al., 2015a)
syd-2(ok217)	~2 Kb deletion covering most of the N-terminal coiled coil domains. Results in a frame shift and stop codon at amino acid 200 (out of 1139 amino acids total).	Behavioral phenotypes and PCR with primers inside deleted region	*C. elegans* Gene Knockout Consortium and (Kittelmann et al., 2013; Wagner et al., 2009)
unc-10(md1117)	Deletion of entire unc-10 coding region.	PCR with primers inside deleted region	(Koushika et al., 2001)

Table S3. Transgenic arrays

Array name	Insertion location in the genome	Experimental contents and injection concentrations	Co-transformation markers and injection concentrations	References for transgene or integrated insertion
ceEx461	extrachromosomal array	KG#796 [strn-1::GFP] (25 ng/ μl)	None	This study
ceEx469	extrachromosomal array	KG#802 [unc-17::STRN-1-Hs cDNA] (4 ng/ μl)	pPD118.33 [myo-2::GFP] (0.75 ng/ μl)	This study
ceEx480	extrachromosomal array	KG#817 [unc-17::STRN-1 cDNA] (4 ng/ μl)	pPD118.33 [myo-2::GFP] (0.75 ng/ μl)	This study
ceEx489	extrachromosomal array	KG#838 [unc-17::SAD-1a cDNA] (4 ng/ μl)	pPD118.33 [myo-2::GFP] (0.75 ng/ μl)	This study
ceIs123	I: ~13.31	KG#367 [unc-129::GFP] (5 ng/ μl)	KG#255 [ttx-3::RFP] (25 ng/ μl)	(Hoover et al., 2014)
ceIs201	I: center	KG#686 [unc-17::INS-22-Venus] (6 ng/ μl) KG#654 [unc-17::ssmCherry] (4 ng/ μl) KG#248 [unc-17::mCherry] (4 ng/ μl)	KG#381 [myo-2::RFP] (1.5 ng/ μl)	(Hoover et al., 2014)
ceIs255	I: -23 or +21	KG#691 [unc-129::INS-22-Venus] (1.5 ng/ μl) KG#687 [unc-129::ssmCherry] (2.5 ng/ μl) KG#240 [unc-129::mCherry] (2.5 ng/ μl)	KG#255 [ttx-3::RFP] (15 ng/ μl)	(Edwards et al., 2015b)
ceIs308	IV: ~3.4	KG#859 [mig-13::INS-22-Emerald] (5 ng/ μl) KG#500 [mig-13::RFPA] (5 ng/ μl)	KS#4 [odr-1::RFP] (20 ng/ μl)	This study

Table S4. Plasmids

Plasmid name	Brief Description	Cloning details or reference giving cloning details
KG#59	rab-3:: expression vector	(Schade et al., 2005)
KG#94	unc-17:: expression vector	(Edwards et al., 2008)
KG#230	unc-129:: expression vector	(Edwards et al., 2009)
KG#240	unc-129::mCherry	(Edwards et al., 2009)
KG#248	unc-17::mCherry	(Hoover et al., 2014)
KG#255	ttx-3::RFP	(Edwards et al., 2009)
KG#367	unc-129::GFP	(Edwards et al., 2013)
KG#381	myo-2::-RFP	(Hoover et al., 2014)
KG#471	mig-13:: expression vector	(Edwards et al., 2015b)
KG#497	myo-3::mcs-RFPA	(Hoover et al., 2014)
KG#500	mig-13::mcs-RFPA	Used Kpn I/ Apa I to cut out the ~1.0 Kb unc-54 3' control region from KG#230, leaving the 6.1 Kb vector fragment containing the mig-13 promoter. To this vector fragment, we ligated the 1.8 Kb Kpn I/ Apa I fragment (containing RFPA + unc-54 3' control region) cut from KG#497 myo-3::mcs-RFPA.
KG#654	unc-17::ssmCherry	(Hoover et al., 2014)
KG#686	unc-17::INS-22-Venus	(Hoover et al., 2014)
KG#687	unc-129::ssmCherry	(Edwards et al., 2015b)
KG#691	unc-129::INS-22-Venus	(Edwards et al., 2015b)
KG#696	unc-17β::sad-1a cDNA	(Edwards et al., 2015a)
KG#720	rab-3::STRN-1-FLAG cDNA	Used AffinityScript Multiple Temperature Reverse Transcriptase and a primer engineered with a restriction site and FLAG tag to make the strn-1-FLAG cDNA (1470 bp). Used Herculase II polymerase and primers engineered with restriction sites to amplify and clone the cDNA into Nhe I/ Kpn I cut KG#59 (rab-3::___ expression vector; 4.9 Kb).
KG#796	strn-1::GFP	Used Herculase II polymerase and primers engineered with restriction sites to amplify and clone the 3.4 Kb strn-1 (C16E9.2) promoter region from N2 genomic DNA into Pst I/ Sac I cut pPD95.67 (4.5 Kb). The promoter region included the entire intergenic region between the 5' UTR of F14B8.6 (which is in opposite orientation upstream of strn-1) and the 5' UTR of C16E9.2 and also includes the 1st 10 bp of C16E9.2's 5' UTR.
KG#802	unc-17::STRN-1-Hs (Homo sapiens)	Used Herculase II DNA polymerase and primers engineered with restriction sites to amplify and clone the 1.2 Kb strn-1-Hs cDNA (conserved protein KIAA0390) from the Genscript ORF clone ID Ohu03925 into Nhe I/ Kpn I cut KG#94 unc-17:: expression vector (6.9 Kb).
KG#817	unc-17::STRN-1cDNA	Used Herculase II DNA polymerase and primers engineered with restriction sites to amplify and clone the 1470 bp strn-1 cDNA from KG#720 rab-3::strn-1-FLAG cDNA into Nhe I/ Kpn I cut KG#94 (unc-17::___; 6.9 Kb).
KG#838	unc-17::sad-1a cDNA	Use Nhe I/ Kpn I to cut out the 2.7 Kb sad-1a cDNA from KG#696 (unc-17::sad-1a cDNA) and clone it into the like-digested unc-17:: expression vector KG#94 (6.9 Kb).
KG#843	gRNA F&E plasmid for targeting rimb-1 knockout	Designed forward and reverse primers bearing the gRNA site and complimentary overhangs (forward: 5'-TCTTGN_{20}-3' and reverse 5'-AAACN*$_{20}$C-3', where N*$_{20}$ denotes the reverse complement of N_{20}). We began by annealing forward and reverse oligonucleotides and then ligated them into the BsaI – cut vector **pJP118**. We did a Qiagen Tip-20 prep on 1 clone, confirmed the size by restriction digest, and submitted it for sequence with the M13 primer to sequence across the insertion site.
KG#858	ANF-Emerald	Gift of Edwin Levitan, University of Pittsburgh
KG#859	mig-13::INS-22-Emerald	Used Q5 Polymerase and engineered primers to produce overlapping PCR fragments followed by NEBuilder Master Mix to insert the 331 bp INS-22 gene coding region (from N2 genomic DNA) and the 720 bp Emerald fragment (PCRed from KG#858) into the mig-13:: expression vector KG#471 (7.1 Kb).
KS#4	odr-1::RFP	Gift of Kang Shen, Stanford University (Klassen and Shen, 2007)
pDD162	eft-3::Cas9	AddGene
pPD95.67	Promoterless GFP vector with SV40 nuclear localization signal	Gift of Andrew Fire, Stanford University
pPD118.33	myo-2::GFP	Gift of Andrew Fire, Stanford University
pJP118	U6::sgRNA (F+E) (gRNA F+E plasmid)	Gift of Andrew Fire and Joshua Arribere, Stanford University

File S1. Supplemental Materials and Methods and Supplemental Material References

Supplemental Materials and Methods

Growth and mounting of strains for imaging

Strain growth: Young adult progeny that had not previously been starved were grown for imaging as described (Edwards et al., 2015a). Growth times and plating numbers were modified for slow growing or lower fertility strains, such as strains containing *syd-2(ok217)* or *nud-2(ok949)*. ~55 young adults were selected and transferred to an unseeded plate immediately prior to mounting as described below.

Agarose pad slide production: Clean glass slides were produced as described (Edwards et al., 2015a). We produced ~18-19 mm diameter agarose pads, except we standardized the agarose concentration at 4% in M9 buffer as follows. After melting 0.4 g of agarose in 10 mls of M9 in a 50 ml Pyrex bottle (Thermofisher, No. 1395) with the lid screwed as tight as possible, we cooled the bottle on a folded paper towel for 2 min, slowly unscrewed the cap to prevent boiling, and poured 0.5 ml of the molten agarose into up to 10 X 1.5 ml microcentrifuge tubes in a 100° Isotemp block (Fisher) for distribution to clean slides as described, using a method described for standardizing agarose pad slides for time lapse video microscopy (Edwards et al., 2015a).

Mounting animals on agarose pad slides: For static non-time lapse imaging of DCVs, we applied a 30 μl drop of 30 mg/ ml BDM (2, 3-Butanedione monoxime; Sigma B0753) in M9 buffer onto a 24 X 30 mm coverslip. We then transferred the prepicked animals in one pick-full to the drop on the coverslip and incubated them for 10 min, placing the coverslip on a 1.5 cm square pad of folded paper towel tissue under a Petri plate lid. After the incubation, we removed ~19 μl of the solution using a P20 microinjection tip (Eppendorf 5242 956.003), leaving the worms behind in the remaining anesthetic, and inverted the coverslip onto a ~18-19 mm diameter 4% agarose pad that had been dried without its protective coverslip for the final 4 min of the incubation. We imaged animals over the next 35 – 55 min.

Image acquisition and processing

We viewed animals using a Nikon Eclipse Ti-E inverted microscope equipped with a Nikon CFI Apo TIRF 100X/ 1.49 N.A. objective, a Nikon motorized high resolution z-drive, and a motorized filter turret containing GFP, YFP, and Texas Red filter cubes (Semrock). Our illumination source was a SOLA Light Engine LED source (Lumencor). We acquired images with an ORCA Flash 4.0 16-bit camera (Hamamatsu, Bridgewater, NJ) controlled by Metamorph v. 7.7. We controlled exposure times by using Metamorph to turn the LEDs on and off rather than using a shutter. We only collected images from animals with their ventral or dorsal surfaces facing the objective and “center quad” (center quadrant) mode of the camera. Z-series interval sizes (0.312 μm) and plane numbers (16) were the same for all strains and transgenes. Exposure times were identical for different strains in each experiment and chosen to collect at sub-saturating levels. Before imaging each strain, we measured the light power of the peak emission wavelength at the objective using an XR2100 power meter (Lumen Dynamics) and an XP750 objective plane light sensor (Lumen Dynamics) with the stage position set at a standard distance (z-position) from the objective. We then adjusted the percent power of the SOLA Light Engine to produce the targeted mW power for the experiment. We used AutoDeblur Gold CWF (Media Cybernetics) to deconvolve the image stacks using the Adaptive PSF blind method and 10 iterations at the low noise setting. After deconvolving, we used Metamorph to make maximum intensity projections of each image stack.

Quantitative image analysis

We used Metamorph 7.7 for most analysis and quantification. To quantify fluorescence intensities per micron, we used the Trace Region tool to trace the region and used the Multiline tool to obtain the length of the traced region. We then copied and moved the region to a similar "on animal" background region for use in background subtraction. For dorsal axons in *ceIs201* strains, we traced the entire axon length across the image. To trace the dendrite regions around DA6 and DB6 in *ceIs255* strains, we started each of the two dendrite regions at the outer edge of each soma, proceeding outward toward each edge of the image and combining the data from the two dendrite regions. Axonal and dendritic data were logged to a spreadsheet, which subtracted the background and computed the total fluorescence per micron of length. To quantify cell soma intensity per square micron on the maximum projected images in *ceIs201* strains, we traced the somas with the multi-line tool. Where necessary, cell soma boundaries were identified using the cell-filling soluble mCherry channel, and the same boundaries were used to trace images in the INS-22-Venus channel. In some cases, axons from the ventral nerve cord ran over part of the soma. If this was the case, we excluded this section of the soma from the traced region since all values were normalized to unit area. Background regions were subtracted as described above for axons and dendrites. After quantifying an image set, we produced representative images for display by saving an 8-bit version of an image that was close to mean +/- standard error for the set. All representative images within an experiment were scaled identically.

Special imaging methods

Imaging strn-1::GFP transcriptional reporter expression (ceEx461 transgene): To image whole L1 or L3 larvae, animals were immobilized as described above under "Mounting animals…." and imaged using the above-described microscope and camera in full-frame mode (not center quad). For L1s, we used a 40X oil, 1.3 Numerical Aperture objective, acquiring 20 z-planes at 0.7 μm intervals using 7 mS exposure times through the GFP filter set. Images were processed by deconvolution as described above in "Processing Images". For L3s, we used a 20X dry, 0.75 Numerical Aperture objective, acquiring 18 z-planes at 1.0 μm intervals using 10 mS exposure times through the GFP filter set. Images were processed by deconvolution as described above in "Processing Images".

Imaging DCVs in the DA9 synaptic and distal asynaptic regions: To obtain high resolution images of DCVs in the entire DA9 dorsal axon (~500 microns in length), we acquired ~3 overlapping full-frame images (designated a, b, and c) spanning from the posterior bend of the axon through to the first commissure that intersects with the DA9 asynaptic region (which ends just posterior to the vulva). DCVs were marked in DA9 with the neuropeptide cargo INS-22-Emerald using the *ceIs308* genomically-integrated transgenic array. We used exposure times of 20 mS (GFP filter) and 2 mS (Texas Red filter). Images were processed by deconvolution as described above. To quantify the synaptic region, we used the trace region tool in Metamorph to trace the brightest 40 micron part of the synaptic region (and a corresponding "on animal" background region). In ventrally oriented animals, we traced the DA9 soma, avoiding the nearby VA12 soma. To determine the start of the asynaptic region, we first determined the longest synaptic region length in 15 wild type image sets. To do this, we opened the first (most posterior) "a" wild type image in the first set of overlapping images. We used the multi-line tool to trace the DA9 axon from the center of the posterior commissure bend in the tail through the synaptic region to last DCV punctum that precedes a gap of >= 6 μm. If there was no such gap in the "a" image in the set, we traced to the edge of the image, opened the overlapping "b" image, identified the region of overlap, and continued tracing until we reached a gap of >= 6 μm between DCV puncta, adding the 2 lengths from the "a" and "b" images. We repeated this for all 15 wild type image sets and noted the longest wild type synaptic region length. This length was the starting point for counting DCVs in the asynaptic region in both wild type and mutants. To count DCVs in the asynaptic region, we counted all DCVs detectable above background, from the start of the asynaptic region through to the point at which the first fluorescently-labeled commissure intersects with the DA9 axon, proceeded through all 3 overlapping images in each set and tracking the axon length and number of DCVs in each image. Overlapping images were aligned using landmarks in the

axon and animal. Scaling was adjusted as necessary to detect all DCV puncta above background. An Excel workbook accepted the a, b, and c lengths and DCV numbers, added them together for total length and total number and then determine DCV number/ micron and the mean, standard deviation, and standard error of the mean.

Profile plots of DCV fluorescence in the DA9 axon: To plot the DCV fluorescence distribution in DA9, we used the Plot Profile module of Image J. We used the segmented line tool with a line width of 20 pixels to trace along the length of the axon in each of 3 overlapping images comprising the DA9 axon (see above). We started at the posterior bend and ended at the point where the first fluorescently labeled commissure intersects with the DA9 axon. We created profile plots from each of the 3 overlapping images in the set. The Y-axis maximum was set to the highest Y value in the 3 overlapping images of the set. We then copied the plot values into a SigmaPlot workbook. We saved the SigmaPlot graphs (one for each of the 3 overlapping images of the set) as JPEGs, imported them into Canvas and cropped them. We then used Object > Scale to shrink the vertical dimension and expand the horizontal dimension. The 3 graphs were further cropped and merged together at their points of overlap to make a single high resolution profile plot comprising the entire DA9 dorsal axon.

Counting DCVs in the axon initial segment: We used ventral soma images acquired from strains containing *ceIs201*. These images contained multiple somas with commissures (axon initial segments) extending toward the dorsal cord. We counted DCVs in any commissures that were in the field of view and in focus from the edge of the soma to the point where it crosses one of the sublateral axon tracks running longitudinally down the animal. We used the line tool to click along the commissure and determine its length. We then simply counted all of the DCV puncta in each commissure. Any puncta that were distinguishable above background were considered countable. Puncta positioned close to each other were counted as multiple if cleavage between the puncta could be distinguished. From previous time lapse studies, and the time lapse experiments in the current study, we have determined that most such puncta in the axon initial segment represent individual DCVs since DCVs are not known to be transported in clusters.

Immunostaining of formaldehyde-fixed animals

Freeze cracking and fixing animals: We prepared freeze-cracked 4% paraformaldehyde fixed, young adult worms for immunostaining as described (Charlie et al., 2006a), with the exception that we modified the freeze cracking procedure as follows to prevent the fixative from freezing during freeze cracking. Steps before and after freeze cracking were identical to the above published procedures. To freeze crack worms, we filled one 50 ml conical per strain with 40 mls of 4% formaldehyde in 1X PBS, pH 7.4. The fixative was made fresh by breaking a 10 ml ampule of 16% formaldhyde (Ted Pella EM grade #NC9658705) and mixing its contents with 26 mls of ddH2O and 4 mls of 10X PBS in a 50 ml conical. The 50 ml conical with fixative was immersed in ice for at least 45 min. Freshly frozen slide sandwiches containing ~1500 young and mature adults sandwiched between two overlapping glass slides were prepared as described (Charlie et al., 2006a; Charlie et al., 2006b). Then, up to 12 such sandwiches were successively cracked and combined with cold fixative as follows. At time 0 sec, a count-up timer was started. The first slide sandwich was removed from its dry ice block, and the two slides of the first sandwich were vigorously separated and laid, worm-side-up on a styrofoam surface at room temperature for 1:30 min. At 1:20 – 1:30 min, the second slide sandwich was cracked and laid next to the first two halves on the styrofoam surface. From 1:30 min – 2:45 min, the two halves of the first sandwich were placed back-to-back and immersed in the ice cold fixative in the 50 ml conical tube, using forceps to hold the slides. The worms were rinsed off of both slides forcefully using a P1000 pipet, and then the rinsed slides were discarded. The third sandwich was then cracked at 2:50 – 3:00 min, followed by rinsing worms from the second sandwich at 3:00 – 4:15, etc. until all the worms from 2 – 12 sandwiches have been rinsed into the cold fixative. The worms were then concentrated by pouring ~1/3rd of the suspension into a 15 ml conical, spinning 2000 rpm for 10 sec in a swinging bucket rotor in a Dynac clinical centrifuge at room temperature with the brake applied, removing the supernatant with vacuum suction, and

repeating twice more. We left ~ 1 ml after the 3rd spin, and then used a Pasteur Pipet or P1000 to forcefully rinse off any animals stuck to the bottom of the tube and transfer the suspension into a 1.5 ml snap-cap tube. We then spun this tube at 6000 rpm for 12 sec in a microfuge, removed most of the cold fixative, and replaced it with 1 ml of previously reserved room temperature fixative. All subsequent steps (30 min fixation at room temperature, quenching in 1 ml of 0.1M glycine, pH 7.4 for 5 min, washing with Antibody Buffer B, blocking with 3% BSA block, and staining with primary and secondary antibodies, and post-staining washes) were performed as described (Charlie et al., 2006a; Charlie et al., 2006b). For immunostaining of EGL-21 dense core vesicles we used Rabbit anti-EGL-21 primary antibody (1/200; KM39A-5.1) (Hoover et al., 2014). The secondary antibody was Goat anti-Rabbit Dylight 550 (Pierce). We used a Semrock Cy3 filter set to view the Dylight 550 signal.

Imaging animals: We used the same microscope, objective, light power monitoring system, and acquisition software described above for live animal imaging. We imaged well-filleted animals that had their dorsal cords exposed and oriented toward the objective. Any such region of the dorsal cord except the first or last 15% was chosen for imaging. Z-stacks of 20 images separated by 0.2 μm were collected.

Image processing and quantification: We processed, deconvolved, quantified, and chose representative images as described above for live animal imaging.

Time lapse microscopy (axon initial segment)

Growth of strains: Animals were grown to the young adult stage as described above for quantitative fluorescence imaging, except we used as many as 30-40 locomotion plates to provide sufficient numbers of animals for the many time lapse mountings.

Agarose pad slide production: We prepared agarose pad slides as above. Slides were stored at 4° and used fresh the next day.

Mounting animals on slides: We first equilibrated the agarose pad slides at room temperature in their humidified container and prepared fresh 6 mM Levamisole in M9 from a powder stock of Levamisole (Acros Organics; AC187870100; <6 months old). To mount animals on a pad, we pre-picked 30-40 young adults to an unseeded plate, applied 30 μl of 6 mM levamisole to a 24 X 30 mm coverslip, picked the 30 young adults to the droplet in one pick-full, and incubated them for 6:10 min on a moist Kimwipe square under a Petri plate lid. Immediately after picking the worms to the drop, we removed the coverslip from one of the agarose pad slides and added 10 μl of M9 + 6 mM Levamisole to the coverslip, and then re-applied the coverslip to the pad, leaving it on the pad until ~40 sec remained on the count-down timer. When removing the coverslip we also removed as much of the 10 μl as possible along with the coverslip by tilting the coverslip up as soon as it slides off the pad and dragging the liquid away from the pad. We then blotted around the edge of the pad with a Kimwipe to remove excess liquid. When the 6:10 timer finished, we put the coverslip back on the Petri plate lid (wiping the moisture off of the part that contacted the wet Kimwipe square first) and removed 23.5 - 25.5 μl of liquid (average 24.5, but adjusted as needed depending on pad size and wetness after removing the M9) by pipetting while viewing under the stereomicroscope. We used a gel loading tip inserted onto a P20 set on the desired volume to remove the liquid in one attempt. When applying the new coverslip with worms face down onto the pad, we used a pair of jeweler's forceps to gently lower it onto the pad. On properly mounted coverslips, a small amount of liquid should wick across in all directions and slightly overflow the pad.

Image acquisition: We acquired images using the same microscope, camera, and computer system described above. We adjusted the light power of a SOLA LED light engine to 25% (a good level for reducing bleaching without compromising signal when using the YFP filter and the *ceIs201* transgene). We mounted the slide on the microscope and scanned the pad left to right, top to bottom using transmitted light and DIC optics to find the first animal oriented with its ventral cord facing the objective. Using the YFP filter, we then focused on the cholinergic motor neuron commissures ~halfway between the central and posterior part of the animal and positioned the stage to allow

viewing of the soma and 2-3 commissures. At 5:30 min after applying the coverslip, we started the first time lapse and continued collecting for 45 sec. Each time lapse consisted of 115 frames collected at 394 msec intervals, with an exposure time of 50 msec for each frame. We used the "center quad" mode of the camera. If possible, one additional time lapse was collected from a different animal, starting within 1:15 min of finishing the first time lapse. However, no more than 2 time lapses were collected per slide. During each time lapse, the focus was adjusted as needed to optimize the focus of the 1 – 3 visible commissures.

Processing time lapse images and converting them to kymographs: We used the Review Multidimensional Data Metamorph plug-in to convert the time lapse images into a multi-image TIFF file. We then used the Multi-line tool to trace along the center of the axon initial segment, starting at the cell soma boundary and proceeding outward. During tracing we moved back and forth between tracing and the slider such that we could visualize the precise path as INS-22-Venus DCV puncta moved through the axon (i.e. following the puncta by clicking as they move along the axon). After ending the trace, we used the Kymograph plug-in to set the line width at a value that included all of the puncta throughout the movie. If animal movement shifted the axon's position slightly during the movie, we adjusted the line width to the minimum width that allowed all puncta along the commissure to be included in the boundaries (up to ~30 pixels maximum). We then created, reviewed, and saved the Kymograph, used the Save Regions plug-in to save the line traces associated with the file, and noted the optimal line width for each trace.

Quantifying movements and percent of time spent paused from kymographs: After opening the multi-plane tiff file in Metamorph, we used the Load Regions plug-in to re-load the line traces, and set the line width at the above determined optimum. We then re-created the kymograph (in Metamorph, previously saved kymographs can't be used to log data). We analyzed each punctum separately and traced its movements with the line tool set on specific colors for each movement state as follows: anterograde (green), retrograde (red), and paused (yellow). Then, if the punctum was not visible for the entire kymograph, we drew a light blue line covering the total time that the punctum was visible.

Pauses were analyzed on all time lapses having at least 58 frames. The key to pause analysis is to create a separate region file for each punctum in the commissure. To start, we chose one punctum to analyze and traced each movement and pause using the line tool and the above color code. We always traced the punctum's pauses last, after tracing anterograde and retrograde movements. In crowded commissures it was helpful to switch between the kymograph and the original multi-plane tiff file to follow movements. If 2 puncta merge and then split off again, we assumed that each punctum maintained its original direction. We then saved this region as a .rgn file appended with "-pause-xx", where xx denotes a sequential number for each puncta in the commissure. We then logged the pause data, selecting Time as the only outputted measurement. We deleted each yellow pause line as we logged it, and then logged the blue "total time visible" line last. The red and green lines were not logged or deleted at this point. We then repeated this procedure for the rest of the puncta in the commissure, successively building a new region file for each new punctum.

Each new region file started with the anterograde and retrograde movements of all previous puncta in the commissure. We then added the movements and pauses for the next puncta as above, logged and deleted the next puncta's pauses, etc. until the region file for the last punctum in the commissure was created. The final region file thus contained all of the anterograde and retrograde movements for all puncta in the commissure, with all of the yellow pause lines deleted because they have been logged. Our Excel Workbook calculated mean, standard deviation, and standard error of the % of time each puncta spent in a paused state. Calculations were performed in a "combined" fashion (grouped by commissure) and in an "uncombined" fashion (all puncta measurements pooled together). We then logged all anterograde data for the commissure by successively logging and deleting each green line. We finished by logging all retrograde data for the commissure by successively logging and deleting each red line. Our Excel spreadsheet then calculated the average run lengths and velocities in each direction in a "combined" fashion (grouped by commissure) and in

an “uncombined” fashion (all puncta measurements pooled together). The above steps were repeated for each commissure’s kymograph.

Definition of a movement: A “movement” was defined as occurring when a punctum moves at a velocity of >= 0.35 microns/ sec for a time of >= 0.90 sec (for short movements that last 0.90 – 3.0 seconds) or a velocity of >= 0.075 microns/ sec for a time of >= 3.0 seconds. A movement continues until it pauses for >= 1 seconds or until it reverses direction, or until it reaches the end of the time course, or until it merges with another punctum and does not reappear out the other side. Movements that changed their velocity without pausing or changing direction were treated as single point-to-point straight line movements, with one end of the line at the beginning of the movement and the other end at the end of the movement (thus creating an average distance and time from point A to point B).

Time lapse microscopy (DA9 movement analysis in densest 40 microns and proximal flux analysis)

Growth of strains: Animals were grown to the young adult stage as described above for quantitative fluorescence imaging, except we used 15 locomotion plates per strain to provide sufficient numbers of animals for time lapse slide mountings.

Agarose pad slide production: We prepared agarose pad slides as above. Slides were stored at 4° and used fresh the next day.

Preparation of Muscimol for immobilization: We used 20 mM Muscimol for immobilization. We found that this $GABA_A$ receptor agonist better immobilized animals for time lapses as compared to 6 mM Levamisole. Mounted animals have straight postures and are more likely to be oriented with a vertical dorsal-ventral axis. Axons showed robust axonal transport during the 15 min mounting time. Although we did not routinely recover animals after these time lapses, in separate experiments we found that animals immobilized in Muscimol recovered within 10-15 min after rescuing from slides versus ~6h after immobilizing in Levamisole. To prepare 20 mM Muscimol, we dispensed the ~10 mg of the stock bottle (Tocris 0289/10) onto a tared piece of weigh paper, obtained a precise weight, and dissolved it in ddH2O at a concentration of 20 mM. We then froze 60 μl aliquots in 200 μl PCR tubes and stored them at -85° until the day of use.

Mounting animals on slides: We first equilibrated the agarose pad slides at room temperature in their humidified container and thawed the required number of 20 mM Muscimol aliquots. To mount animals on a pad, we pre-picked ~25-35 young adult animals (0 – 3 eggs OK) to an unseeded plate. At the appropriate time (mountings were spaced at 15 min intervals in a timed schedule), we added a 30 ul drop of 20 mM Muscimol to a coverslip and picked all of the animals from the unseeded plate to the drop. 12 min after starting this incubation, we slid the protective coverslip from an agarose pad and allowed the pad to pre-dry for ~3:00-4:00 min. 15 min after starting the incubation, we withdrew the optimal volume of liquid (typically 18.75 ul) and inverted the coverslip onto the pad, lowering gently with jeweler’s forceps. No nail polish was added. On properly mounted coverslips, a small amount of liquid should wick across in all directions and slightly overflow the pad. We then placed the slide coverslip-down on an edge-side-up Petri lid and marked the animal positions with a fresh fine-point sharpie. The slide was then delivered to a second person to perform the time lapse imaging and so on, following a timetable of delivering a fresh slide every 15 min.

Image acquisition: We acquired images using the same microscope, camera, and computer system described above. We adjusted the light power of a SOLA LED light engine to 28% (a good level for reducing bleaching without compromising signal when using the GFP filter and the *ceIs308* transgene). We mounted the slide on the microscope and used a flashlight to align the stage such that the objective was under the first animal’s position (marked above with a black dot). We then checked the animal’s position using DIC transmitted light though the eyepieces and determined if it was oriented dorsally toward the objective. If not, we used a flashlight to align the stage with the next animal’s black-dotted position. If an animal was dorsally oriented, we used the Texas Red filter to focus on the DA9 axon, approximately centering the synaptic region in the field of view and used the

mCherry-filled boutons as a guideline for the synaptic region. At 3:00 min after receiving the slide, the microscopist started the first time lapse and continued collecting for 45 sec, adjusting the focus manually during the time lapse as needed. Each time lapse consisted of 115 frames collected at 394 msec intervals, with an exposure time of 30 msec for each frame. We used the full-frame mode of the camera. If possible, up to 3 additional time lapses were collected from different animals, starting within 12 min of receiving the slide. This process was repeated for up to 21 additional slides for up to 88 time lapses total per strain.

Image processing and analysis: We converted each set of 115 time lapse images into a multi-image TIFF file using the Review Multidimensional Data Metamorph plug-in of Metamorph. We produced Kymographs of the full synaptic region plus a flanking proximal region back to the posterior bend (see Time Lapse Microscopy: axon initial segment for general method of producing Kymographs). Despite technical challenges of this experiment due to the relatively high DCV population density in this region (~10 per micron on average in wild type), we were able to clearly visualize DCV movements. Several factors, including the brightness of individual Emerald-labeled DCVs, the ability to adjust the scaling of the 16-bit images over a wide range to permit contrast with closely positioned stationary DCVs, and the presence of many spaces between the relatively small DCV clusters, contributed to the success of this experiment. For movement analysis in the densest 40 microns, we drew a 40 micron line on the Kymograph that marked the most dense region (determined by eye). We then analyzed DCV movements using methods as above (Time Lapse Microscopy: axon initial segment), except that percent of time spent paused was not analyzed. If, during movement, the DCV crossed in front of or behind one or more stationary DCVs, such that its path was obscured for a period of time, the movement was assumed to continue uninterrupted if the DCV emerged with the same speed and trajectory on the other side. “Movement” was defined as a punctum moving a distance of >= 1.00 microns at a velocity of >= 0.6 microns/ sec. If a punctum paused for >= 1.18 (3 frames) seconds or reversed direction, then the movement was considered complete and any new movement of that punctum was considered a different movement. Scaling of the kymograph was adjusted manually frequently/ constantly during analysis, and occasionally the original multi-image Tiff file was consulted to maximize information for determining the beginning or end of a movement. In most cases, precise beginning and ending points could be determined within the limits of 1 apparent (diffraction-limited) DCV diameter by using appropriate scaling. In a few cases, when a precise beginning or end point could not be observed due to a large cluster of stationary DCVs, the beginning or end of the movement was designated as edge of the cluster closest to where movement was first or last observed. Movements had to begin or end in the 40 micron test region to be counted. We analyzed the entire length of the movement. Thus, the movement could begin or end outside the 40 micron region. This was possible because the camera’s field of view showed extensive flanking regions (~35 microns on each side). For the flux analysis proximal to the synaptic region, we simply designated a line in a vesicle-free space ~7 microns prior to the beginning of the synaptic region and counted the number of puncta crossing this line in each direction.

Supplemental References

Ackley, B.D., Harrington, R.J., Hudson, M.L., Williams, L., Kenyon, C.J., Chisholm, A.D., and Jin, Y. (2005). The two isoforms of the Caenorhabditis elegans leukocyte-common antigen related receptor tyrosine phosphatase PTP-3 function independently in axon guidance and synapse formation. J Neurosci *25*, 7517-7528.

Blumenthal, T. Trans-splicing and operons in C. elegans. In WormBook, T.C.e.R. Community, ed. (WormBook).

Blumenthal, T., and Steward, K. (1997). RNA Processing and Gene Structure. In *C elegans* II, D.H. Riddle, T. Blumenthal, B.J. Meyer, and J.R. Priess, eds. (Cold Spring Harbor Laboratory Press), pp. 117-145.
Charlie, N.K., Schade, M.A., Thomure, A.M., and Miller, K.G. (2006a). Presynaptic UNC-31 (CAPS) is required to activate the G alpha(s) pathway of the Caenorhabditis elegans synaptic signaling network. Genetics *172*, 943-961.
Charlie, N.K., Thomure, A.M., Schade, M.A., and Miller, K.G. (2006b). The Dunce cAMP phosphodiesterase PDE-4 negatively regulates G alpha(s)-dependent and G alpha(s)-independent cAMP pools in the Caenorhabditis elegans synaptic signaling network. Genetics *173*, 111-130.
Deken, S.L., Vincent, R., Hadwiger, G., Liu, Q., Wang, Z.W., and Nonet, M.L. (2005). Redundant localization mechanisms of RIM and ELKS in Caenorhabditis elegans. J Neurosci *25*, 5975-5983.
Edwards, S.L., Charlie, N.K., Milfort, M.C., Brown, B.S., Gravlin, C.N., Knecht, J.E., and Miller, K.G. (2008). A novel molecular solution for ultraviolet light detection in Caenorhabditis elegans. PLoS Biol *6*, e198.
Edwards, S.L., Charlie, N.K., Richmond, J.E., Hegermann, J., Eimer, S., and Miller, K.G. (2009). Impaired dense core vesicle maturation in Caenorhabditis elegans mutants lacking Rab2. J Cell Biol *186*, 881-895.
Edwards, S.L., Morrison, L.M., Yorks, R.M., Hoover, C.M., Boominathan, S., and Miller, K.G. (2015a). UNC-16 (JIP3) Acts Through Synapse-Assembly Proteins to Inhibit the Active Transport of Cell Soma Organelles to Caenorhabditis elegans Motor Neuron Axons. Genetics *201*, 117-141.
Edwards, S.L., Yorks, R.M., Morrison, L.M., Hoover, C.M., and Miller, K.G. (2015b). Synapse-Assembly Proteins Maintain Synaptic Vesicle Cluster Stability and Regulate Synaptic Vesicle Transport in Caenorhabditis elegans. Genetics *201*, 91-116.
Edwards, S.L., Yu, S.C., Hoover, C.M., Phillips, B.C., Richmond, J.E., and Miller, K.G. (2013). An organelle gatekeeper function for Caenorhabditis elegans UNC-16 (JIP3) at the axon initial segment. Genetics *194*, 143-161.
Ferguson, E.L., and Horvitz, H.R. (1985). Identification and characterization of 22 genes that affect the vulval cell lineages of the nematode Caenorhabditis elegans. Genetics *110*, 17-72.
Fridolfsson, H.N., Ly, N., Meyerzon, M., and Starr, D.A. (2010). UNC-83 coordinates kinesin-1 and dynein activities at the nuclear envelope during nuclear migration. Dev Biol *338*, 237-250.
Hoover, C.M., Edwards, S.L., Yu, S.C., Kittelmann, M., Richmond, J.E., Eimer, S., Yorks, R.M., and Miller, K.G. (2014). A Novel CaM Kinase II Pathway Controls the Location of Neuropeptide Release from Caenorhabditis elegans Motor Neurons. Genetics *196*, 745-765.
Kittelmann, M., Hegermann, J., Goncharov, A., Taru, H., Ellisman, M.H., Richmond, J.E., Jin, Y., and Eimer, S. (2013). Liprin-alpha/SYD-2 determines the size of dense projections in presynaptic active zones in C. elegans. J Cell Biol *203*, 849-863.
Klassen, M.P., and Shen, K. (2007). Wnt signaling positions neuromuscular connectivity by inhibiting synapse formation in *C. elegans*. Cell *130*, 704-716.
Koushika, S.P., Richmond, J.E., Hadwiger, G., Weimer, R.M., Jorgensen, E.M., and Nonet, M.L. (2001). A post-docking role for active zone protein Rim. Nat Neurosci *4*, 997-1005.
Patel, M.R., Lehrman, E.K., Poon, V.Y., Crump, J.G., Zhen, M., Bargmann, C.I., and Shen, K. (2006). Hierarchical assembly of presynaptic components in defined C. elegans synapses. Nat Neurosci *9*, 1488-1498.
Schade, M.A., Reynolds, N.K., Dollins, C.M., and Miller, K.G. (2005). Mutations that rescue the paralysis of Caenorhabditis elegans ric-8 (synembryn) mutants activate the G alpha(s) pathway and define a third major branch of the synaptic signaling network. Genetics *169*, 631-649.
Wagner, O.I., Esposito, A., Kohler, B., Chen, C.W., Shen, C.P., Wu, G.H., Butkevich, E., Mandalapu, S., Wenzel, D., Wouters, F.S.*, et al.* (2009). Synaptic scaffolding protein SYD-2 clusters and activates kinesin-3 UNC-104 in C. elegans. Proc Natl Acad Sci U S A *106*, 19605-19610.
Weimer, R.M. (2006). Preservation of C. elegans tissue via high-pressure freezing and freeze-substitution for ultrastructural analysis and immunocytochemistry. Methods Mol Biol *351*, 203-221.

White, J.G., Southgate, E., Thomson, J.N., and Brenner, S. (1986). The Structure of the Nervous System of the Nematode *Caenorhabditis elegans*. Phil Trans R Soc Lond *314*, 1-340.